Proceedings, 7th African Rift Geothermal Conference
Kigali, Rwanda 31st October – 2nd November 2018

Three-dimensional geophysical modelling of Kiejo-Mbaka geothermal field, Tanzania

Daniele Rizzello[1], Egidio Armadillo[2], Claudio Pasqua[3], Paolo Pisani[3], Taramaeli Mnjokava[4], Jonas Mwano[4], Didas Makoye[4], Lucas Tumbu[4]

1) Tellus s.a.s., Italy. 2) DISTAV, Universita' di Genova, Italy. 3) ELC-Electroconsult s.p.a, Italy. 4) Tanzania Geothermal Development Company Ltd (TGDC), Tanzania.

rizzello@tellus-explora.eu;egidio@dipteris.unige.it;claudio.pasqua@elc-electroconsult.com;paolo.pisani@elc-electroconsult.com;
taramaeli.mnjokava@tanesco.co.tz;jonas.mwano@tanesco.co.tz;
makoye.didas@tanesco.co.tz; lucas.tumbu@tanesco.co.tz

Key words: Kiejo-Mbaka, magnetotellurics, gravity, 3D modelling.

ABSTRACT

The Kiejo-Mbaka geothermal field is located close to the eastern margin of the Karonga Rift Basin and is part of the Rungwe volcanic province where the EARS splits up into its Western and Eastern branches in southern Tanzania. The area is characterised by a Precambrian gneiss metamorphic basement complex, outcropping along the NW-trending, SW-dipping Mbaka fault. Geothermal manifestations mainly consist of hot springs, flowing close to the Mbaka fault. An integrated geophysical survey was carried out over the Kiejo-Mbaka geothermal field by TGDC (Tanzania Geothermal Development Company), under the supervision of ELC-Electroconsult (Italy). The campaign included 76 Magnetotelluric (MT) and Transient Electromagnetic (TEM) soundings and 133 gravity measurements; a dense station grid allowed for a detailed geophysical 2D and 3D modelling. Two and 3D gravity modelling indicate that the positive residual Bouguer anomaly can be explained by a high density (3 g/cm^3) body, constituting the gneiss basement, elongating NW-SE. NE and SW of it, lower density layers (2.5 g/cm^3) are observable; the attitude of their bottoms is compatible with the Mbaka fault direction and the Livingstone fault trend (NNW). We found that 3D MT inversion was the only tool giving a reliable resistivity imaging in the Mbaka prospect. From the final 3D MT model, a very resistive body (>2000 Ohm m) deepening toward SE is visible; this body represent the gneiss basement, and the surfaces delimiting it are associated with the Mbaka fault and the Livingstone fault trend. Three conductive zones (less than 10 Ohm m) have been identified: two of them affect the Mbaka fault footwall, NE of the resistive basement, while another one is located beneath the plain, SE of it. This latter zone shows a thickness of about 1 km. It is apparent that the low-density regions well correspond with the high-conductivity zones imaged by the MT 3D inversion. The integrated geophysical interpretation then leads to two possible geological scenarios: these regions can be constituted by (post-rift) sediments (possibly affected by

low-T geothermal alteration) or by intensively fractured and low-T altered basement; however, we stress that the possible geothermal alteration is not necessarily related to the present-day geothermal activity, and caution should be taken in result interpretation.

1. Introduction

Magnetotelluric (MT), time domain electromagnetic (TDEM) and gravity surveys were carried out in the Kiejo-Mbaka (Tanzania) geothermal prospect in the period September 19, 2016 - October 31, 2016, by TGDC (Tanzania Geothermal Development Company) and Tellus (Italy), under the supervision of ELC-Electroconsult (Italy).

The objective of the survey was to acquire high-resolution gravity and MT/TDEM data in order to obtain a model of the subsurface resistivity and thus provide additional constraints for the set-up of the relevant conceptual model. The optimised acquisition layout allowed to a reliable 3-D geophysical modelling. The campaign was funded by the Icelandic International Development Agency (ICEIDA) and the Nordic Development Fund (NDF), with the aim to support geothermal exploration and capacity building in East Africa, as part of the Geothermal Exploration Project (GEP).

As far as we know, our survey constitutes the first detailed geophysical exploration accomplished over the Kiejo-Mbaka area. Only a regional gravimetric survey of the Karonga Basin has been reported by Ebinger et al. (1993).

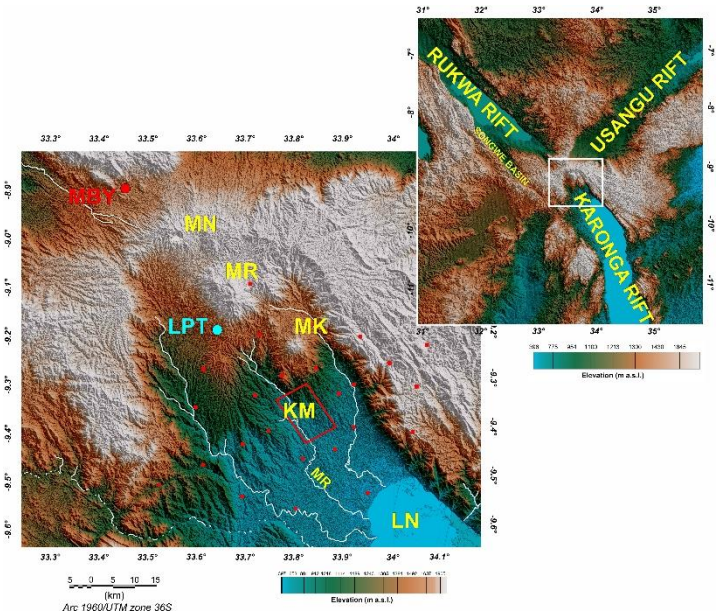

Figure 1: Location of the Kiejo-Mbaka survey area in the Karonga Rift. KM: Kiejo-Mbaka area (marked by a red rectangle); RVP: Rungwe Volcanic Province; MK: Mount Kiejo; MR: Mount Rungwe; MN: Mount Ngozi; MR: Mbaka River. LN: Lake Nyasa. Town of Mbeya is marked by MBY (red circle). The MT reference site (Lupoto) is labelled "LPT". The red dots indicate the regional gravity stations. Main rivers are marked by blueish lines.

2. Geological settings

The Kiejo-Mbaka geothermal area is located close to the eastern margin of the Karonga Rift (see Fig. 1), and it's part of the Rungwe volcanic province of the Western Rift branch of the East African Rift System. The basaltic and volcaniclastic sequence from the Rungwe covers accommodation zones between the Songwe, Usangu and Karonga asymmetric basins. The Sogwe Basin is a rift valley linking the Rukwa depression to the Rungwe Volcanic Province (Delvaux et al., 2013). The beginning of Karonga rifting is dated late Miocene – Pliocene, and its volcanism and faulting propagated from S to N after 7 Ma to present; the volcanics aren't older than about 8 Ma (Ebinger, 1993).

The oldest formation outcropping in the area is the *Precambrian Livingstone Gneiss*, overlain by the *metamorphic and intrusive complex* ("MIT"), constituted by meta-anorthositic and amphibolitic complex. More recent formations are the *Karonga volcanics* (Basaltic Lavas), the *sedimentary basement* (Pliocene-Pleistocene siltstones and sandstones) and the *Lake Nyasa lacustrine deposits* (Pleistocene stratified clays). Youngest volcanics are the *Katete Trachitic-Phonolitic Ignimbrite* and the *Tukuyu basalts.*

The tectonic setting is dominated by the *Mbaka fault trend* (N130-140°), constituting the graben NE master fault, superimposed on the *Livingstone rift fault trend (N120°)*. Secondary trends come from the superposition of the *Lake Nyasa rift* (N-S) and the *Usangu rift trend* (N030-040°) tectonics.

In the Kiejo-Mbaka area the geothermal manifestations are constituted by the Kilambo hot springs (64°C), and the Lufundo fossil fumaroles. The estimated reservoir temperature is about 140°C (ELC, 2017b). The geological map (from ELC, 2017a) is displayed in Fig.2.

3. The geophysical survey

A comprehensive view of the geophysical layout is given in Figure 2. Magnetotellurics and TDEM measurements were carried out by TGDC personnel at 76 stations, located along 8 profiles, with a station spacing of 750 m. A more detailed sampling was set around the Kilambo geothermal springs. A gravity survey consisting of 108 stations were performed, with a nominal spacing of 700 m along 9 lines. Twenty-five additional stations have been acquired up to at a distance of about 30 km around the prospect (Fig.1), in order to evaluate the regional gravity field.

3.1 MT and TDEM investigations

Three Phoenix V5 System MT equipments acquired EM data in the 1000-0.0001 Hz range. One station located in Lupoto, about 20 km away from the survey area (Fig. 1), served as remote reference. Average record length was 26.3 hrs. Proprietary software was used to estimate the MT impedance and geomagnetic tipper by combining the remote reference technique (Gamble et al., 1979) and robust MT processing (Sutarno, 2008). The resulting impedance and tipper resulted of good quality, thanks to the very low noise

in the area and good field practice. The MT static shift was corrected by means of joint inversion of MT phase and TDEM apparent resistivity data, providing the two apparent resistivity correcting factors (s_{xy}, s_{yx}). Joint inversion was carried out by means of the Meju (1996) approach.

The MT impedance was corrected by the following linear relationship,

$$Zc = C\ Zd \qquad (1)$$

where, $\boldsymbol{C}$ is a diagonal matrix which elements are the correcting factors, and $\boldsymbol{Z_d}$ and $\boldsymbol{Z_c}$ are the distorted and corrected impedance, respectively.

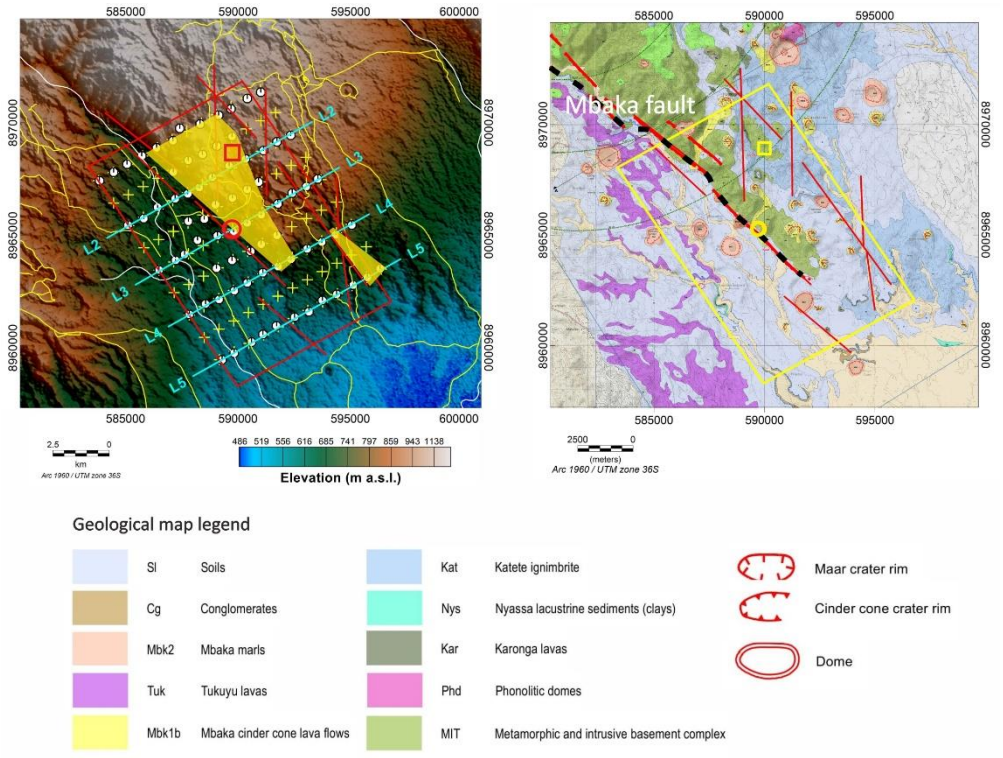

Figure 2: Left: geophysical stations. White circles, MT/TDEM points, yellow crosses, gravity stations. The Kilambo hot springs are marked by a red circle, while the Lufundo manifestations by a red square. White lines indicate the main rivers, and yellow lines mark the main roads. The shaded yellow polygons are the areas where out-of-quadrant MT phase occurs (see text). Right: geological map of the area (from ELC, 2017a).

One-dimensional inversion revealed inadequate for most of the stations due to ubiquitous strong 3D conditions. Furthermore, many stations showed an out-of-quadrant phase (>90°) in the yx-mode (see Fig.3). This occurred along a NW-SE elongated central zone (see Fig.2). Qualitatively, this phenomenon could be due the strong current channelling produced by high resistivity contrasts (see e.g. Ichihara, 2009). For these reasons, we therefore chose to perform a 3D inversion of the MT dataset. Another cause could be electrical anisotropy (see e.g. Heise, 2003), but investigating this possibility was beyond our initial aim.

Three-dimensional inversion has been carried out by means of the ModEM software, a FD software designed for parallel computing (Meqbel, 2009; Egbert and Kelbert, 2012; Kelbert et al., 2014).

We inverted the full (unrotated) and static shift - corrected impedance tensor (Z), jointly with Tz from the whole dataset, using 19 periods between 0.003 s and 1000s.

We assigned error floors of 10% of $|(Zxy\ Zyx)|^{0.5}$ to the Zxy and Zyx impedance tensor components, and 20% of $|(Zxy\ Zyx)|^{0.5}$ for Zxx and Zyy. A value of 0.05 was used as error floor for the tipper components. Heavily biased or scattered data were manually discarded after inspection.

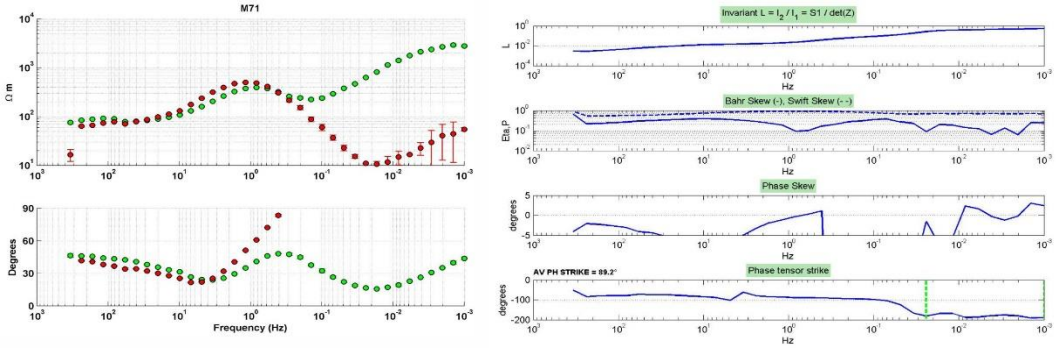

Figure 3: Example of station with phase (yx) exceeding 90° (MT71). Left: MT curves (red dots: yx mode; green dots: xy mode). Right: dimensional parameters indicating strong 3D conditions

The 3D grid consists of 58 X 58 X 55 cells in x – y and z – directions. In the central portion, the horizontal cell size is 450 m. At shallow depth, the minimum height of each cell is 50 m. The cell width increases logarithmically towards the edges of the model, and with depth. With the aim to validate the results, different initial models were used. Our preferred model derived from the initial model obtained from the Tz inversion started from a 100 Ohm m half-space. As an example of data fit, Figure 4 shows the response at station M71.

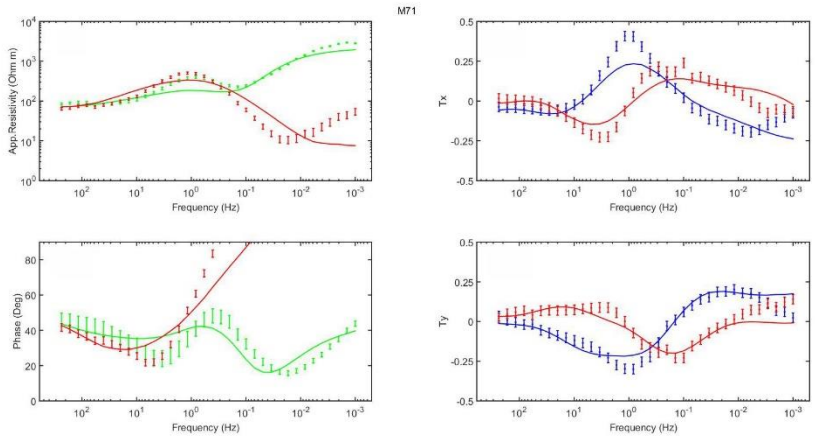

Figure 4: Data fit from 3D inverse modelling at station M71. Left: MT data (red dots: yx mode; green dots: xy mode). Right: Tx and Ty components of the tipper data (blue: real component; red: imaginary).

3.1.1 Results of MT data inversion

The most significant resistivity slices extracted from the 3D model are displayed in Figure 5; the main visible features are the following:

- A resistive (100-1,000 Ohm m) nucleus ("R") dominates the central portion of the survey area and corresponds to the outcropping basement. It is delimited by discontinuities D1 and D2 (identified by the 100 Ohm m isoresistive). The basement widening at depth reflects the SW dip of the Mbaka fault and the NE dip of D2. Between 0 and 200 m a.s.l., a resistive anomaly (50 Ohm m) is visible (C4); given its resistivity it could represent a high-T alteration zone.
- West of the Mbaka fault resistivity of about 100 Ohm m at shallow depths, agrees with the shallow Tukuyu Basalts. Starting from 200 a.s.l., a conductive zone C1 appears (0.5 - 15 Ohm m).
- On the eastern side of the Mbaka fault two conductive zones C2 and C3 are visible. The first one appears to be related to the Lufundo fumaroles at the shallowest depth.

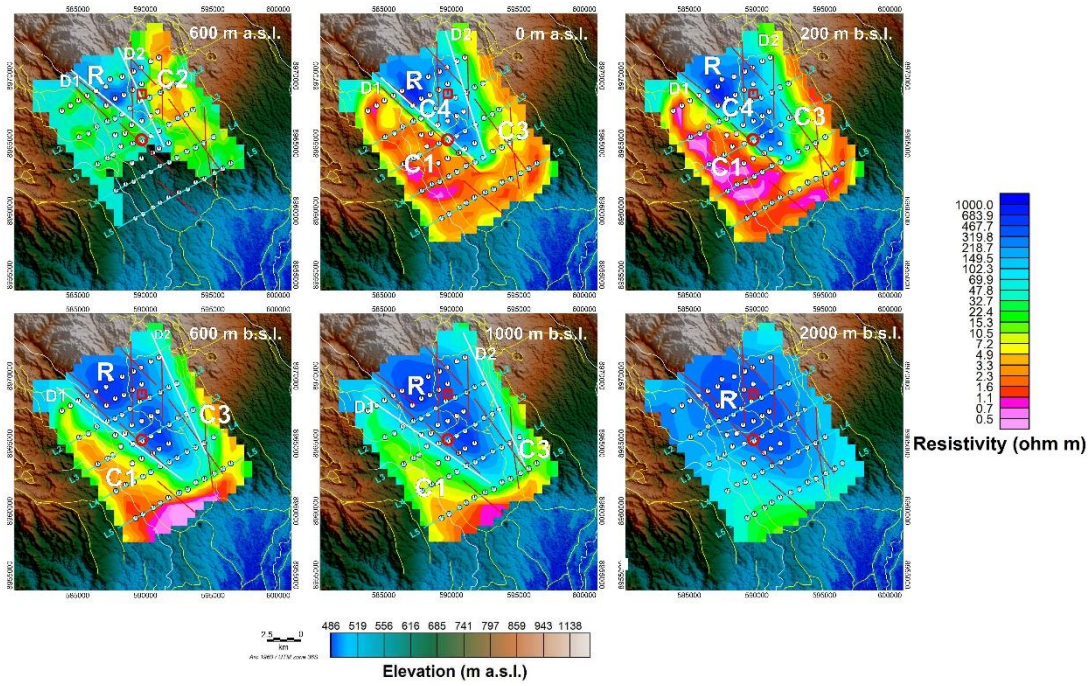

Figure 5: Horizontal slices of the 3D model from 800 m to -2000 m a.s.l. White circles: MT stations. Red circle: Kilambo hot springs; red square: Lufundo fumaroles. White straight lines indicate the inferred lineaments. The main resistivity features are labelled by "R", C1", "C2", "C3" and C4. White lines indicate the main rivers, while yellow lines the main roads.

Four resistivity cross-sections from the 3D model along profiles L2, L3, L4, L5 are displayed in Figure 6, from which it can be observed that:

- The central resistive core ("R") corresponding with the outcropping MIT basement, deepening from section L2 to L5.

- The C1 anomaly thickens toward SW and SE (800-1000 m). This support the hypothesis of (conductive) sediment accumulation, with a possible contribution from the Nyasa Lake. On the other hand, this layer could include geothermally low-T altered portions of the metamorphic basement.
- Profile L2 confirms that C2 could be associated with the Lufundo fossil geothermal manifestations and represent paleo-geothermal alteration. The anomaly might represent a low-T alteration zone. However, its thickness increases toward the Nyasa Lake and it seem to connect with anomaly C1 (section L5), suggesting the presence of lacustrine sediments.
- The discontinuity D1 is associated to the Mbaka fault, but their position doesn't match at surface. This indicates non-tectonic factors govern the resistivity distribution. Thus, it seems that low-T alteration affects also the Mbaka fault foot wall. The discontinuity D2 marks a border between the resistive rift shoulder (R) and the conductive zones toward East (C2 and C3).

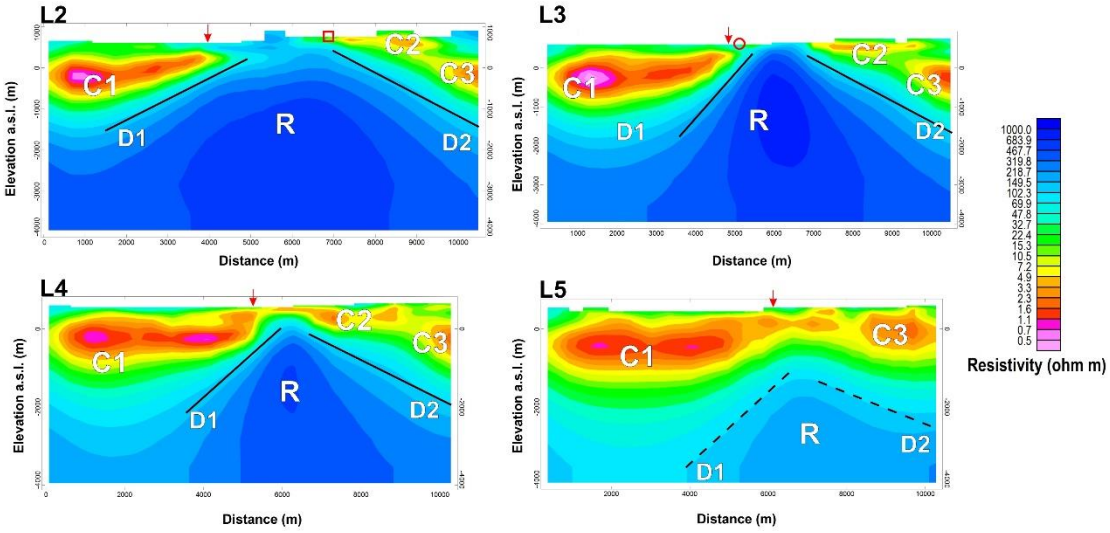

Figure 6: Resistivity cross-sections L2, L3, L4 and L5. The red circle indicates the location of the Kilambo manifestations, the red square the Lufundo fumaroles. The red arrow marks the Mbaka fault trace.

3.2 The gravity survey

Gravity measurements were carried out by a G927 LaCoste & Romberg meter equipped with electronic beam, levels and feedback system. Data were acquired in combination with differential GPS positioning, which allowed to a vertical precision <0.1 m for most of the stations. Corrections for scale factor, tide, drift, latitude, free air, Bouguer and topography were applied.

To estimate the reference density for Bouguer and topographic corrections, we have used both direct and indirect methods. Direct measurements of density were carried out in laboratory at the University of Genoa, and provided values comprised between 2,500 and 3,050 kg/m^3 for the Precambrian Metamorphic Complex. At the same time, the classical approach of Parasnis (1951) was applied, providing a density of 3,000 kg/m^3; this value was therefore adopted for the final Bouguer anomaly computation.

The regional gravity field has been estimated by means of 25 'regional' stations acquired around the survey area (see Fig. 1). The field has been obtained by gridding the Bouguer anomaly over the 'regional' stations and a subset of the stations of the detailed grid (Fig. 7). The obtained values are similar to those shown by Ebinger et al. (1993) in their profile AA' (pag.17,822). The residual Bouguer map is shown in Figure 8.

3.2.1 2D Modelling

The main Bouguer anomalies to be modelled are the high anomaly values trending NW and the corresponding low values that border the gravimetric high (labelled "H" and "L" in Fig. 8). In the following 2D models, we have assumed that the higher residual Bouguer anomaly values in the "H" area are due to the metamorphic basement high density.

The same density has been assumed to characterize the basement in the whole survey area.

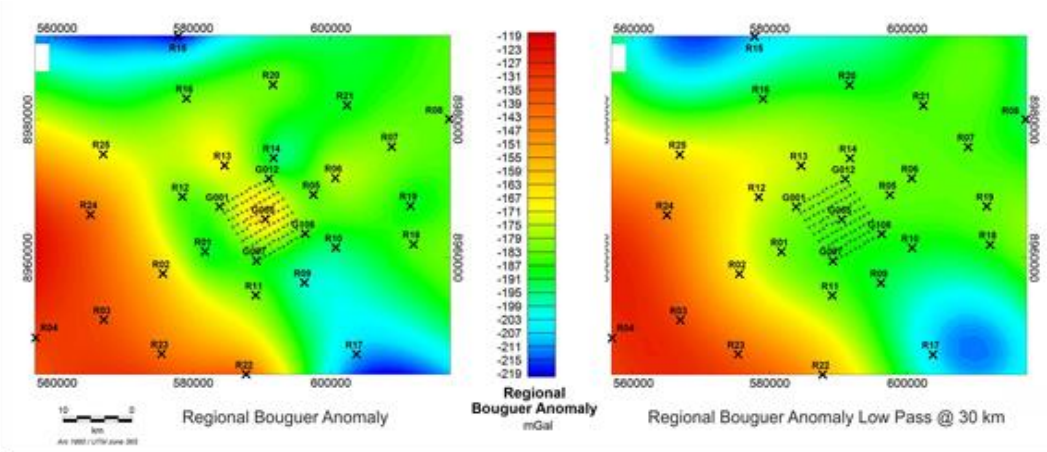

Figure 7: Left: the regional Bouguer anomaly map computed from the 'regional' stations and the local stations of the detailed survey. Right: low pass of the regional Bouguer anomaly map with wave-length cut-off at 30 km. The large black crosses represent the location of regional gravity stations. The small crosses indicate the detailed gravity survey area. The low pass map is assumed to represent the regional field over the survey area (see the small crosses). The reference density for the Bouguer anomaly is 3,000 kg/m^3.

Forward tests indicate that the Tukuyu lavas and/or the Katete ignimbrites cannot explain the gravimetric lows 'L', due to their small thickness (as inferred from the geological survey). We have then hypothesized a large region of lower density. Due to the lack of information about of this layer, we have assumed that it may correspond to the low resistivity anomalies shown in Figure 6.

We have verified that a density of 2,500 kg/m^3 gives a low-density layer thickness that approximatively corresponds to the low resistivity regions. Therefore, we have assumed the existence of anomalous zones, with a density contrast of -500 kg/m^3 with respect to the basement rock assumed at 3,000 kg/m^3. These low-density zones could be ascribed to argillification regions in the basement or to sedimentary accumulation around the uplifted basement block; a mixture of the two contributions is also possible.

Here we show the results of the 2D forward modelling along the profiles L2, L3, L4 and L5 (Fig. 9). For each profile, the corresponding resistivity section is superimposed.

The central anomaly high of each profile is explained by the basement and is associated to high resistivity values. The anomaly lows are explained by low-density layers (2,500 kg/m^3); the thin Tukuyu lavas and the Katete ignimbrites included in these layers cannot be distinguished. The thickness of the low-density region is higher in the SW sector of the profiles, where it has a mean value of 1,500, while in the NE sector is 1,200 m.

3.2.2 3D Modelling

The 3D gravity inversion was carried out by means of the Geosoft GMSYS-3D software. The model is defined by stacked surfaces defining layers with uniform density.

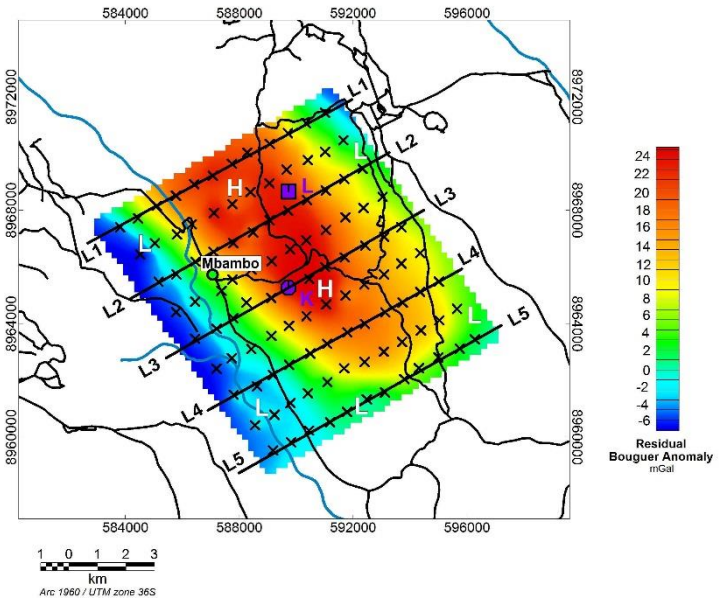

Figure 8: Residual Bouguer anomaly map at 3,000 kg/m^3. Black crosses represent measurement point locations. Large violet square and circle: Lufundo (L) fossil and Kilambo (K) manifestations respectively. Grey and light blue lines: main roads and rivers.

Calculations are performed in the wave number domain accordingly to the R.L.Parker's algorithm (Parker, 1972). Topography was derived from the ASTER DEM, de-sampled at 100 m. Below the surface, we have considered a simple layer with density of -500 kg/m^3 representing the low-density medium.

The bottom of this layer is a horizontal plane at a depth of 0 m. Below this plane, we have assumed the unaltered basement at 0 kg/m^3. The model bottom has been set at 2,000 m b.s.l. During the inversion, the density contrast of -500 kg/m^3 is kept constant. The software then modified the starting plane surface at 0 m elevation in order to get the best data fit.

We have inverted the residual Bouguer Anomaly (Fig. 8). The inverted surface is shown in Figure 10 as an elevation grid a.s.l. The gravimetric bedrock can be approximated by two different planes separated by the Mbaka fault.

The plane to the South West of the Mbaka fault has direction N134°E dipping towards SW with mean inclination 35°. It has the same direction of the Mbaka fault. The plane to the North East has direction N154°E dipping towards NE with mean inclination 14°. Its direction is comparable with the Livingstone trend.

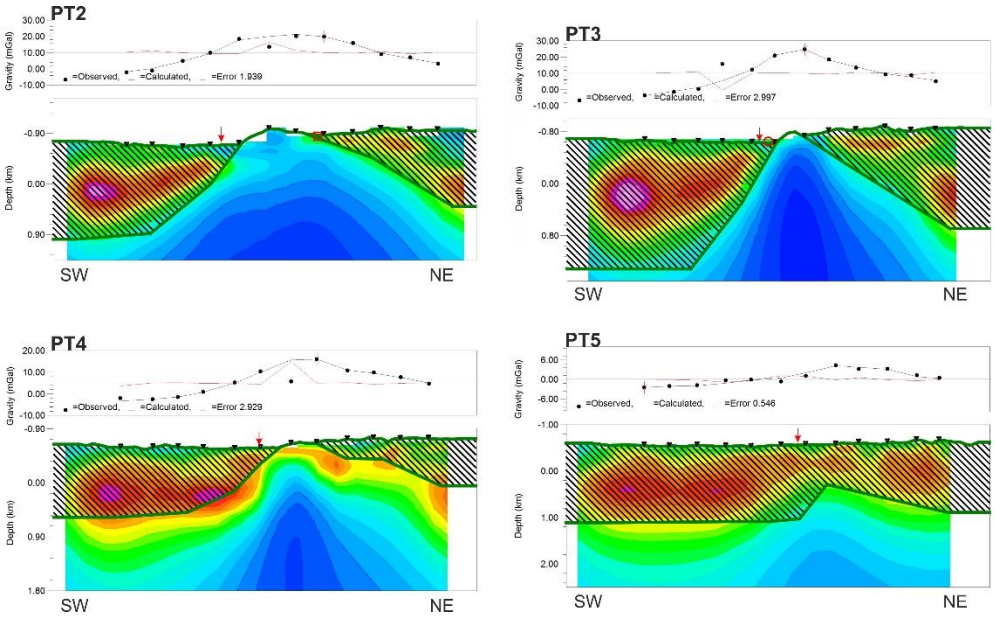

Figure 9: 2D gravity forward modelling along profile L2, L3, L4 and L5. Upper panel of each profile: observed (black dots) vs calculated gravity (black continuous line); red line: error. Lower panel of each profile: 2D density model superimposed on the resistivity sections from the 3D resistivity model (see Figure 7 for the colour palette); no dashed area: basement at 3,000 kg/m^3; dashed area: low-density regions (2,500 kg/m^3).

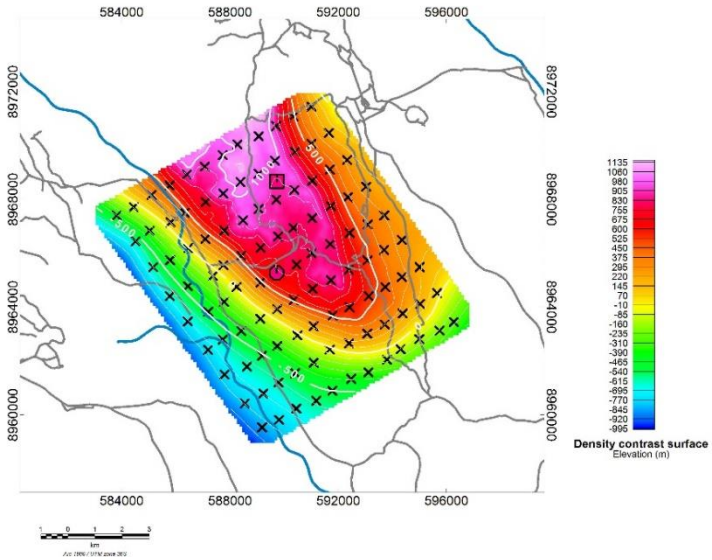

Figure 10: Elevation of the surface separating the unaltered MIT basement from the overlying low-density regions, retrieved from the 3D inversion (white contour lines). Large red square and circle: Lufundo fossil and Kilambo manifestations respectively. Grey and light blue lines: main roads and rivers.

4. Conclusions

The integration of gravimetric and magnetotelluric surveys and the associated advanced 3D interpretation techniques has aided the characterization of the Kiejo-Mbaka geothermal prospect.

Magnetotelluric data exhibited strong 3D conditions and out-of quadrant phase for the yx-mode. However, three-dimensional MT modelling was able to explain the data within an acceptable misfit.

Further work would be addressed to better understand and this phenomenon in the Kiejo-Mbaka prospect. A resistive nucleus (100-1,000 Ohm m), confidently interpreted as the metamorphic basement was imaged. This feature is surrounded by conductive regions (1-10 Ohm m), on the plain south west of the Mbaka fault, and on the graben shoulder.

Gravity processing indicated that a very high density should be attributed to the metamorphic basement (3,000 kg/m^3).

The gravity high occurred in correspondence of the basement uplifted block, limited by two surfaces coherent with the Mbaka and Livingstone faults. Around it, toward SW and NE, gravity lows were observed (2,500 kg/m^3).

The conductive anomalies are well correlated with the low-density regions. This led to hypothesize that these zones can have been interested by low-T geothermal alteration, developed in the basement or could be the geophysical signature of sedimentary covers, originated from the basement uplift (and a possible contribution from the Nyasa Lake). A local combination of the two hypothesis is also possible.

Future possible geoscientific works on the Kiejo-Mbaka area should include additional MT/TDEM and gravity stations toward SW and NE. This would help to understand the real extension and shape of the conductive and less dense regions, with the aim to enlighten their origin.

AKNOWLEDGEMENTS

This work was founded funded by the Icelandic International Development Agency (ICEIDA) and the Nordic Development Fund (NDF). The Tanzania Geothermal Development Company (TGDC), ELC-Electroconsult, Tellus s.a.s. and the Department of Earth, Environment and Life Sciences of the University of Genoa (DISTAV) provided instrumental and technical support.

REFERENCES

Delvaux, D., Temu, E.B., Deino, A., Kraml M. "Tectonic evolution of the Rukwa rift basin and interaction with the Rungwe Volcanic Province", Western Tanzania. *24rd Colloquium of African Geology,* Addis Ababa, Ethiopia, January 8-14, 2013. Abstract Volume, p. 123.

Ebinger, C.J., Deino, A.L., Drake, R.E., Tesha A.L., Becker T., Ring U. "Tectonic Controls on Rift Basin Morphology: Evolution of the Northern Malawi (Nyasa) Rift." *Journal of Geophysical Research* (1993), vol. 98, no. B10, pages 17,821-17, 836.

Egbert, G.D. & Kelbert, A. "Computational recipes for electromagnetic inverse problems". *Geophys. J. Int.*,189(1), (2012), 251-267.

ELC Electroconsult (a). *Kiejo-Mbaka Geological Report* (Milan, Italy, unpublished, 2017).

ELC Electroconsult (b). *Kiejo-Mbaka Geochemical Report* (Milan, Italy unpublished, 2017).

Gamble, T.D., Goubau, W.M., Clarke, J. "Magnetotellurics with a remote magnetic reference". *Geophysics*, 44, (1979) 53-68.

Ichihara, H., Mogi, T. "A realistic 3-D resistivity model explaining anomalous large magnetotelluric phases: The L-shape conductor model". *Geophys. J. Int*. 179, (2009) 171-176.

Kelbert, A, Meqbel N, Egbert GD, Tandon K. "ModEM: A modular system for inversion of electromagnetic geophysical data". *Computers & Geosciences*, 66, (2014), 40-53.

Heise, W., Pous, J. "Anomalous phases exceeding 90 degrees in magnetotellurics: anisotropic model studies and a field example, *Geophys. J. Int.*, 155, (2003), 308–318.

Meju, M. "Joint inversion of TEM and distorted MT soundings: some effective practical considerations". *Geophysics*, 61, (1996) pp. 56-65.

Meqbel, N. "The electrical conductivity structure of the Dead Sea Basin derived from 2D and 3D inversion of magnetotelluric data". *PhD thesis* (2009), Free University of Berlin, Berlin, Germany.

Parasnis, D.S. "A study of rock densities in the English Midlands". *Roy. Astr. Soc., Geophys. Suppl*., 6, (1951),252-71.

Parker, R.L. "The Rapid Calculations of Potential Anomalies". *Geophys. J. R. Astr. Soc.* 31, (1972), 447-455.

Sutarno, D. "Constrained robust estimation of magnetotelluric impedance functions based on a bounded-influence regression M-estimator and the Hilbert transform". *Nonlin. Processes Geophys.*, 15, (2008), 287-293.